Journal of Power Sources 289 (2015) 91–99

Contents lists available at ScienceDirect

Journal of Power Sources

journal homepage: www.elsevier.com/locate/jpowsour

Cast and 3D printed ion exchange membranes for monolithic microbial fuel cell fabrication

Hemma Philamore [a, *], Jonathan Rossiter [a], Peter Walters [c], Jonathan Winfield [b], Ioannis Ieropoulos [b, *]

[a] Dept. of Engineering Mathematics, University of Bristol, Tyndall Avenue, Bristol BS8 1TH, UK
[b] Bristol BioEnergy Centre, Bristol Robotics Laboratory, University of the West of England, Coldharbour Lane, Bristol BS16 1QY, UK
[c] Centre for Fine Print Research, University of the West of England, Bower Ashton Campus, Bristol BS3 2JT, UK

HIGHLIGHTS

- 3D printed polymer membranes produce power in MFCs.
- Natural rubber latex achieves similar power output to conventionally used membranes.
- Microscopy shows evidence of bacterial degradation/resistance to biofouling.
- pH and conductivity of anolyte play a significant role in performance of MFCs.
- Novel polymer membranes cost less than conventional cation exchange membrane.

ARTICLE INFO

Article history:
Received 16 December 2014
Received in revised form
13 April 2015
Accepted 17 April 2015

Keywords:
Microbial fuel cell
3D printing
Ion-exchange membrane
Oxygen-diffusion cathodes

ABSTRACT

We present novel solutions to a key challenge in microbial fuel cell (MFC) technology; greater power density through increased relative surface area of the ion exchange membrane that separates the anode and cathode electrodes. The first use of a 3D printed polymer and a cast latex membrane are compared to a conventionally used cation exchange membrane. These new techniques significantly expand the geometric versatility available to ion exchange membranes in MFCs, which may be instrumental in answering challenges in the design of MFCs including miniaturisation, cost and ease of fabrication.

Under electrical load conditions selected for optimal power transfer, peak power production (mean 10 batch feeds) was 11.39 μW (CEM), 10.51 μW (latex) and 0.92 μW (Tangoplus). Change in conductivity and pH of anolyte were correlated with MFC power production. Digital and environmental scanning electron microscopy show structural changes to and biological precipitation on membrane materials following long term use in an MFC. The cost of the novel membranes was lower than the conventional CEM. The efficacy of two novel membranes for ion exchange indicates that further characterisation of these materials and their fabrication techniques, shows great potential to significantly increase the range and type of MFCs that can be produced.

© 2015 The Authors. Published by Elsevier B.V. This is an open access article under the CC BY license (http://creativecommons.org/licenses/by/4.0/).

1. Introduction

The emergence of MFC as a promising renewable energy technology is dependent on optimisation strategies to maximise the power generated using such devices. The theoretical maximum redox potential generated by an MFC is 1.14 V [1], with real systems producing operating voltages significantly lower than this. Proposed strategies for voltage multiplication such as stacking MFCs [2], have driven an increased need for miniaturisation and low cost, rapid fabrication of multiple units, in the design of MFCs. Additionally, past studies have identified one of the greatest challenges in MFC technology as being the design of scalable architectures with large surface areas for oxygen reduction at the cathode and bacteria growth on the anode resulting in higher power density [3]. However, versatility of the design of systems addressing these needs is severely limited by the materials currently used for the ion exchange membrane in an MFC.

* Corresponding authors.
E-mail addresses: hemma.philamore@bristol.ac.uk (H. Philamore), ioannis.ieropoulos@brl.ac.uk (I. Ieropoulos).

http://dx.doi.org/10.1016/j.jpowsour.2015.04.113
0378-7753/© 2015 The Authors. Published by Elsevier B.V. This is an open access article under the CC BY license (http://creativecommons.org/licenses/by/4.0/).

The ion exchange membrane electrically isolates the anode and cathode electrodes while facilitating the proton transport necessary for the redox reaction that generates the cell potential, with the exception of single chamber MFCs which use distal electrodes for this separation. Furthermore, it maximises the coulombic efficiency of the MFC by preventing oxygen diffusion to the anode electrode. Most MFC technology relies on the use of expensive commercial membranes such as Nafion (Dupont) and cation exchange membranes (CEM) which are designed for chemical fuel cells. The planar form of these materials provides low geometric versatility in the design of MFC architectures. Previous work has shown that for a fixed electrode size and anode chamber volume, power density of MFCs scales with ion exchange surface area [3]. Past research has attributed enlarged specific area of the ion exchange surface, facilitating greater ionic conductivity, to a decrease in MFC internal resistance, resulting in higher power density [4] and [5], with areas smaller than that of the electrodes significantly increasing MFC internal resistance [6]. This is particularly applicable to small MFCs which may be preferable when stacking multiple units.

Hence, 3D printed and cast, ionically conductive, monolithic structures present a natural solution to the challenges of increasing the specific ion exchange area for a given anode chamber volume and reducing the overall dimensions of the MFC by decreasing the need for supporting structural material. New ion exchange membrane materials with rapid fabrication processes such as casting and 3D printing significantly expands the range of possible MFC geometries and improves the ease of fabrication and assembly of multiple units.

Recent research has demonstrated the ability of novel, soft materials such as latex condom [7] to exceed the power output of conventional CEM membranes in conventional two chamber analytical style MFCs. Furthermore, functionality of materials such as pre-fabricated latex gloves [8] and cast ceramics [9] for ion exchange and simultaneous structural support has increased the scope of available MFC geometries. Fabrication techniques available to latex such as casting could be used to further expand the range of available architectures beyond those of commercially available pre-fabricated components (condoms and gloves) investigated previously. Cast latex could be used to produce MFCs with high geometric versatility, high power output, fast production rate and optimal materials properties such as high fracture and impact tolerance, and low cost and environmental impact. Hence, this study considers a user-fabricated membrane in contrast to previous studies documenting the use of latex as an IEM.

Nafion is conventionally used as both a membrane in MFCs [10] and as the polymer layer in soft robotic, ionic polymer metal composite (IPMC), actuators [11] due to its ionic conductivity and its function as an electrical insulator. Previous work has documented the use of Tangoplus as a dielectric elastomer (DE) actuator [12], demonstrating the material as an electrical insulator. However, the comparatively low breakdown voltage and small displacements achieved by the actuator compared to polymers more conventionally used as DE actuators suggest the migration of charged particles within the material under electrical stimulus. Hence, by exhibiting similar electro active properties to Nafion, Tangoplus shows potential for use as an ionically conductive electrode separator in an MFC. Furthermore, the hygroscopic nature of the material could be instrumental in providing micro-channels for charged particles to move through. The emergence of 3D printing has made rapid, high precision fabrication of a range of materials, including porous rubber-like polymers such as Tangoplus, widely accessible. Recent work has demonstrated 3D printing as a fabrication method of for complex, novel MFC architectures [13] and electrodes [14]. Hence, the demonstration of a 3D printed polymer as an ion exchange membrane in this study shows that 3D printing can be applied to all components of an MFC and therefore shows the possibility for printing a complete MFC as a single unit.

This study compares the efficacy of two novel materials, Tangoplus 3D printed, acrylic based photo-polymer (Stratasys/Objet Geometries) and natural rubber latex (Tomps) as the ion exchange membrane in a microbial fuel cell, using a conventional material CMI-7000 (CEM) (Membranes International Inc.) as a control population. The work aims to validate the development of MFC systems using the novel materials and fabrication processes described.

2. Experimental method

2.1. MFC design and materials

The performance of novel proton exchange membranes; Tangoplus 3D printed polymer (thickness 116 μm) and natural rubber latex (thickness 100 μm) was compared to that of conventional CEM (thickness 450 μm). The novel materials were obtained in their liquid form and planar membranes of uniform thickness were user-fabricated either by 3D printing (Tangoplus) or by casting the liquid material over a glass surface and using a K-bar (R K Print) to obtain uniform thickness (natural rubber latex) (Figs. 1 and Fig. 2).

An Eden 350V 3D printer (Stratasys/Objet Geometries) was used to print the Tangoplus membranes by photopolymer jetting. A print head was used to deposit Tangoplus acrylate photopolymer resin (Stratasys/Objet Geometries) in 29 μm thick layers. The resin was rapidly cured using UV light from lamps mounted on the sides of the print head and the build platform was lowered prior to deposition of the next layer, on top of the previous, accumulating to the complete 3D print. A gel-like support material was also printed to provide support for overhanging or complex geometries during the print. This was removed using a water jet on completion of the print.

Approximately 50 ml of liquid natural rubber latex was deposited on a glass surface using a syringe. A K Bar (RK Print), comprising a stainless steel rod with a pattern of identically shaped radial grooves, formed by precision drawn, wire windings, was used to draw the wet material across the glass surface. The spacing of the grooves controlled the wet film thickness and a No. 8 bar was used to obtain a membrane thickness of 100 μm. The material was air-cured.

The cuboid, analytical style MFC anode chamber, previously described in Ref. [15] held 25 mL of anolyte, and was open on one side, where a proton exchange membrane with a projected area of 20 cm^2 was attached (Fig. 3). An open to air cathode, with an area of 20 cm^2, made from conductive latex using a method derived from Ref. [8] was used to maintain a continuous redox reaction without

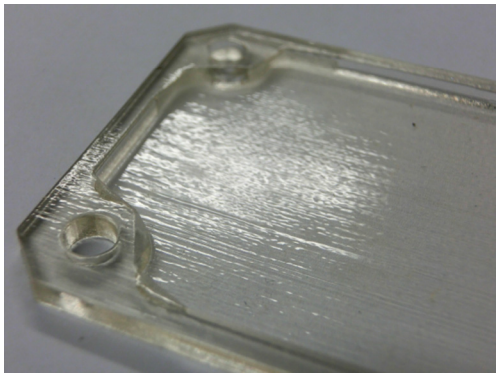

Fig. 1. Tangoplus 3D printed membrane with material grain visible on surface.

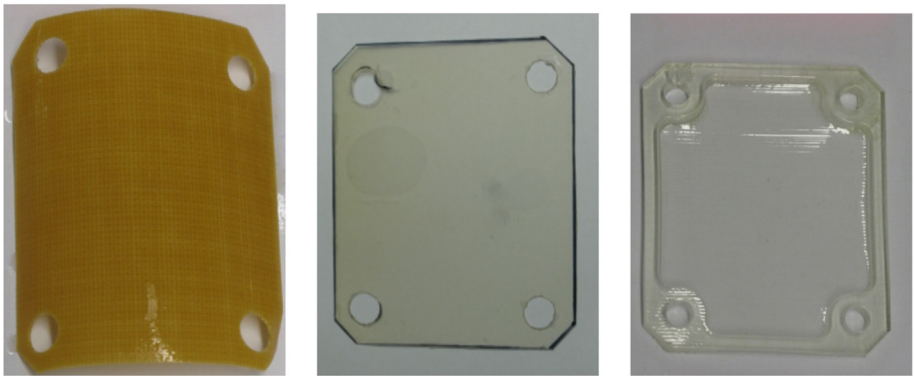

(a) CEM (b) Latex (with acetate support material) (c) Tangoplus (with thicker edge material for sealing/support)

Fig. 2. The three different types of membrane tested.

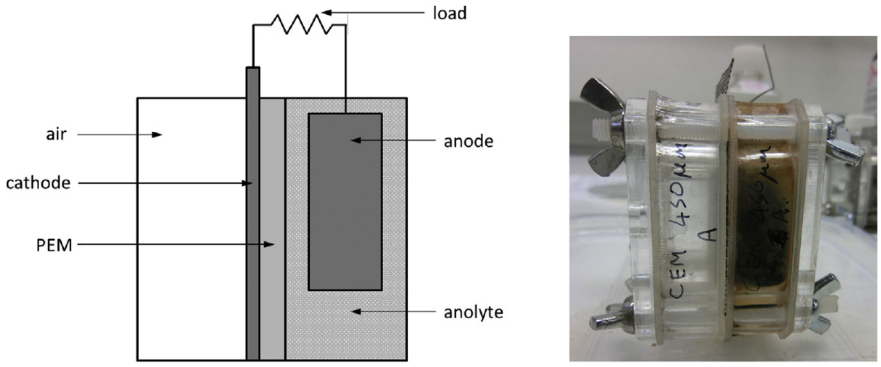

(a) Schematic (b) Photograph

Fig. 3. MFC configuration.

the need to hydrate the cathode electrode. A polyurethane-based rubber coating (Plasti-Dip, Petersfield UK) was mixed with white spirit then micronised graphite powder in the mass ratio 2:3:1, and painted onto the air side of the membrane. Stainless steel mesh was pressed into the un-cured conductive, rubber electrode to provide an electrical connection. The anode electrode was made from carbon fibre veil and had a surface area of 270 cm^2, folded to give a projected area of 7 cm^2. The performance of two replicated systems per membrane material was measured using a Pico Technology ADC-20 data logger.

The cells were inoculated with sewage sludge (Wessex Water, Saltford UK) mixed with nutrient broth (2.5% mass of fluid content) and placed under a 10 kΩ load. 5 ml of fluid was removed daily from the anode chamber and replaced with 5 ml of de-ionised water stock solution with a concentrations 25 mM acetate, mixed with tryptone (1% mass of fluid content) and yeast extract (0.5% mass of fluid content) providing a nutritionally rich medium to promote the growth of bacteria. After two weeks, batch feeding commenced. During a single batch feed the entire contents of the anode chamber of each MFC was evacuated using a syringe and replaced with 25 ml of de-ionised water solution with a concentrations of 5 mM acetate tryptone (0.2% mass of fluid content) yeast extract (0.1% mass of fluid content). The duration of a single batch feed cycle was determined by a drop in power output of the MFCs with conventional CEM to 1 μW (set as the baseline), at which point the anolyte of all MFCs was replenished.

2.2. Load conditions

Over the course of the experiment, the MFCs were examined under three different values of continuous electrical loading with the aim of comparing the different MFC membranes under the load at which they produced maximum power transfer.

After initial inoculation and stabilisation, at 41 days all MFCs were placed under a 1 kΩ load, and their performance examined over a period of 4 weeks (batches 1–4). The 1 kΩ load was selected to imitate the fixed load condition of 950 Ω imposed by a EH4295 Micropower Step Up Low Voltage Booster Module (Advanced Linear Devices), which was selected as an exemplar of state-of-the-art energy harvesting hardware. This was to demonstrate the performance of MFCs under conditions representative of a real world application.

At 89 days, all MFCs were placed under a 4 kΩ load (optimal load for latex, determined from polarisation experiments, Section 2.3), and the difference in performance to the previous 1 kΩ load was observed over a further 17 days (batches 5–6).

In light of the change in power and energy output of MFCs with CEM and latex which accompanied a change in external load from 1 kΩ to 4 kΩ (Section 3), an individual external load was selected for each group of MFCs. At 121 days, individual loads of 1 kΩ (CEM), 3 kΩ (Latex) and 13 kΩ (Tangoplus) were applied to the MFCs for a further 2.5 months, comprising batches 7 to 16, with anolyte replenishment at 8-day intervals. This loading scenario was termed ‘stratified external loading’.

2.3. Polarisation experiments

At 79 days, following batches 1–4 under 1 kΩ load, a polarisation curve was used to find the maximum power point of each MFC and estimate the corresponding applied electrical load. The total anolyte contents of all MFCs were removed and replenished and all MFCs were put under open circuit conditions for one hour prior to the polarisation experiment. Manually operated variable resistors (Centrad Boite A Decades De Resistances) were used to sequentially connect 27 resistances in the range of 40 kΩ to 80 Ω, at 9 min intervals. The time interval was determined from previous work as being sufficient for reaching pseudo-steady-state conditions.

The power produced at each load was calculated by Joule's Law: $P = V^2/R$, where R is a given external load and V is the voltage recorded at that load. Jacobi's law shows that electrical power transfer to a load is maximised where internal reflection losses are minimised, hence the maximum power point occurs where the output resistance of the MFC is impedance matched to the applied external load of the system. Kirchoff's voltage law equates the sum of the potential differences in a closed electrical network to zero. Hence, the internal resistance of each MFC was calculated by: $R_{int} = V_{OC}/I_L - R_{ext}$ where, V_{OC} is the recorded open circuit voltage of the MFC, R_{ext} is the applied load and I_L is the current at that loading, calculated using Ohm's law: $I = V/R$.

At 106 days, following 4 kΩ loading, a second polarisation run was carried out on the MFCs to verify the results of the first. A total of 21 resistances in the range 40 kΩ to 100 Ω, were sequentially connected to the MFCs at 6 min intervals. The new time constant was again selected as the time required to reach pseudo steady-state; this had decreased as a result of maturity.

Optimum load conditions were taken to be the mean of the external resistances at the maximum power point of the two polarisation curves. This produced the optimum load values of 1 kΩ (CEM), 3 kΩ (Latex) and 13 kΩ (Tangoplus).

2.4. Analysis and microscopy

The pH and conductivity of the anolyte was measured (Hanna HI8424 pH meter, Jenway conductivity meter) at the beginning and end of the final batch feed of the experiment.

A 3D Digital Microscope (Hirox) and an environmental scanning electron microscope (Philips XL30 ESEM) were used to view the cross sectional thickness and surface appearance of samples of each membrane material at the beginning and end of the experiment. A razor blade was used to cut orthogonally to the surface of each membrane to obtain a profile of the material cross section. Samples removed from the MFCs at 7 months were rinsed with de-ionised water, and a cotton bud was used to gently remove anolyte residue to expose the surface condition. Prior to viewing using the SEM, all samples were gold sputtered (Emscope SC500). Images were taken from a number of sites on each membrane and the images presented were chosen to best represent the general condition of each sample.

3. Results and discussion

3.1. Performance of MFCs under 1 kΩ load

Under the initial period of continuous 1 kΩ load (batches 1–4) MFCs with CEM show the best performance, with the highest power output (19.67 μW) recorded in batch 4. Latex shows the highest power (7.58 μW, batch 2) of the two MFCs with novel materials, the highest power output from Tangoplus being 0.62 μW, recorded in batch 3.

The polarisation curve produced at 79 days, following batch 4, shows the maximum power point for MFCs with CEM is at an external load of 1 kΩ. The average of the peak power measurement taken for each batch under continuous load exceeds this value (Tables 1 and 2). These data suggest that batches 1–4, under 1 kΩ loading that preceded the polarisation experiment provided optimum power transfer conditions for the CEM based MFCs.

In contrast, MFCs with Latex and Tangoplus membranes show maximum power points during the polarisation experiment at approximately 4 kΩ and 15 kΩ respectively. The peak power produced by one of the MFCs with Tangoplus was approximately double the power produced under the initial period of continuous 1 kΩ loading. This suggests that the continuous 1 kΩ load condition that preceded the polarisation experiment was not the optimal condition for power transfer from these MFCs. The replicate Tangoplus MFC exhibited significantly poorer performance, producing negligible power, hence the exclusion of these data from Fig. 6(a). However consistent performance was observed across all MFCs with Tangoplus membranes in the second polarisation experiment. Significant discrepancy in MFC behaviour during both polarisation experiments was also exhibited between the two MFCs with latex membranes. The more biologically active nature of natural rubber latex compared to the synthetic materials considered (Section 3.5) may have been a cause of variation in system performance. Furthermore, the natural origin of the material may have been a cause of greater variation in the membranes compared with synthetically fabricated materials such as Tangoplus and CEM.

Kirchoff's voltage law shows that energy balance in a closed electrical system is maintained by equating R_{ext} and R_{int}. However, the calculated values of R_{int} (Table 2) are significantly higher than the corresponding external loads. This phenomenon has been noted in previous work [16] and attributed to a dynamic Voc that changes with system parameters, rather than the experimentally derived constant used to calculate the value of R_{int} in Table 1.

3.2. Performance of MFCs under 4 kΩ load

MFCs with CEM show greater peak power output (11.42 μW, average of 2 batches) (Table 1) than those with novel membrane materials under a continuous 4 kΩ load. However, as suggested by the maximum power point during polaristaion (Fig. 6), performance is lower than during batches 1 to 4, at the initial 1 kΩ load (Fig. 4 and Table 1).

MFCs with latex membranes show an increase in peak power (7.56 μW, average of 2 batches) in response to a change in load from 1 kΩ to 4 kΩ. Furthermore, the peak power produced from MFCs with CEM from any single batch feed is within 2 s.f. of the highest of these values (11.94 μW in batch 5), showing good stability of these MFCs at 4 kΩ.

MFCs with Tangoplus membranes also show increased performance in response to an adjustment in load condition from 1 kΩ to 4 kΩ, with peak power output increasing to 1.31 μW (average of 2 batches) (Fig. 4 and Table 1). The greatest power output by MFCs with Tangoplus membranes under continuous 4 kΩ load (1.85 μW) exceeds the maximum power point of both polarisation experiments (1.3 μW (2 s.f.) at 15 kΩ) (Table 2).

3.3. Performance of MFCs under stratified external load

Comparison of the maximum power point on two polarisation curves and their associated load conditions results in the following estimates for the optimal load for maximum power transfer from MFCs of each membrane type (Section 2):

Table 2 summarises the maximum power values identified during the polarisation experiment conducted at 106 days. Both

Table 1
Summary of MFC performance under the three loading regimes; peak power is given as an average of the highest value recorded from each batch feed as well as the overall maximum of the averaged values. Energy is given as an average of the energy produced per batch. 1.

	Load	Batch	Energy(J)	Peak power(μW)	Peak power(μW)
			(Mean of batches)	(Mean of batches)	(Maximum of batches)
CEM	1 kΩ	1–4	5.79	11.70	19.67
	4 kΩ	5–6	5.79	11.42	11.94
	1 kΩ	7–16	5.26	11.39	20.86
Latex	1 kΩ	1–4	0.62	1.21	5.74
	4 kΩ	5–6	1.65	7.56	11.65
	3 kΩ	7–16	2.96	10.51	17.00
Tangoplus	1 kΩ	1–4	0.01	0.14	0.62
	4 kΩ	5–6	0.24	1.31	1.85
	13 kΩ	7–16	0.22	0.92	1.83

Table 2
Summary of MFC performance during polarisation experiments at 79 and 106 days.

	CEM a	CEM b	Tangoplus a	Tangoplus b	Latex a	Latex b
Polarisation at 79 days						
Max power μW	12.67	16.08	0.000007	1.30	0.17	1.17
Max power density μ Wm^{-2} (total anode area)	4692.50	5954.90	0.0027	480.71	61.57	432.67
Max power density μ Wm^{-3} (anolyte volume)	506790.14	643129.60	0.29	51916.32	6649.35	46728.53
External resistance, R_{ext} Ω	1000.00	1000.00	40000.00	15000.00	5000.00	3000.00
OCV mV	437.95	439.25	224.43	388.87	400.32	434.81
Internal resistance, R_{int} Ω	2890.84	2464.10	16659671.95	26805.45	64428.31	19034.38
Polarisation at 106 days						
Max power uW	13.56	12.85	1.33	1.39	1.10	11.71
Max power density μ Wm^{-2} (anode area)	5021.58	4759.72	490.82	513.28	405.62	4337.27
Max power density μ Wm^{-3} (anolyte volume)	542330.94	514050.05	53008.48	55434.33	43806.80	468424.83
External resistance, R_{ext} Ω	1000.00	2000.00	15000.00	15000.00	15000.00	2000.00
OCV mV	437.95	439.25	224.43	388.87	400.32	434.81
Internal resistance, R_{int} Ω	2761.19	3479.65	8876.80	25457.17	31850.70	3682.33

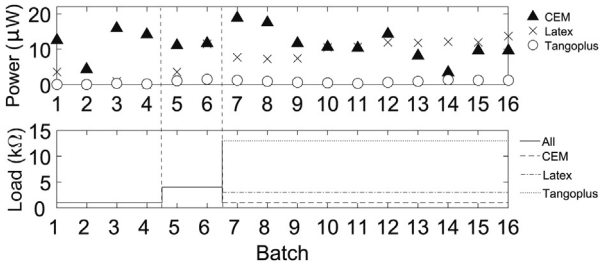

Fig. 4. Peak power per batch (average of two replicate MFCs) at each fixed external load regime.

polarisation experiments, show the maximum power point of MFCs with CEM at 1 kΩ load.

The load at which the maximum power point was shown by MFCs with latex membranes is inconsistent between the two polarisation experiments. The mean of the external resistances that delivered the maximum power output in each experiment is 3 kΩ (1 s.f.).

Similarly, the external load at the maximum power point of MFCs with Tangoplus membranes is inconsistent between the two polarisation experiments. The mean of the external resistances that delivered the maximum power output in each experiment is 13 kΩ (1 s.f.).

MFCs with CEM show the highest performance (average of 10 batches) of the three membrane materials investigated at their stratified loads (Table 1).

In response to returning to 1 kΩ loading (batch 7 onwards), peak power value of MFCs with CEM is higher (11.93 μW when averaged across 10 batches, with the highest being 20.86 μW in batch 7) than at 4 kΩ (batch 5–6) and at the previous stage of 1 kΩ loading (batch 1–4), thereby exhibiting the greatest performance of the three membrane types and a temporal improvement in MFC performance. In contrast, when averaged across batches 7 to 16, at 1 kΩ, power output is lower than the previous 1 kΩ (batches 1–4) and 4 kΩ (batches 5–6) temporal load conditions. This decline in power output per batch indicates temporal deterioration of MFCs with CEM (Fig. 5(a)). This may be attributed to clogging of the membrane over time with biofouling, inhibiting its capability for ion exchange, as described in Ref. [17].

MFCs with latex membrane exhibit their greatest performance under 3 kΩ load (peak power = 10.51 μW, average of 10 batches, with the highest (17.0 μW occurring in batch 12) (Fig. 4). MFCs with latex membrane produced 60% of the average energy output of MFCs compared to conventional membranes loaded at 1 kΩ. Furthermore, in contrast to MFCs with CEM a linear trend of temporally increasing energy production per anolyte replenishment is shown under 3 kΩ demonstrating a longer period of increasing performance and potential for obtaining comparable performance of the novel materials with CEM with long term use (Fig. 5). Previous studies have shown a similar improvement in performance of MFCs with latex membranes [15] and propose biodegradation as a possible factor in improved capability for ionic conduction. The long term operation of these MFCs in the current study and in previous work suggests an improvement in the ionic action of the material as opposed to its use as a carbon source within the MFC bacterial environment.

Inconsistency in the temporal power output from replicate MFCs with CEM and latex membranes is shown under stratified loading conditions. An obvious explanation for the difference in temporal performance of MFCs is that applied loading conditions were not optimised for the whole of the study population. Table 2 shows that maximum power points occurred at significantly

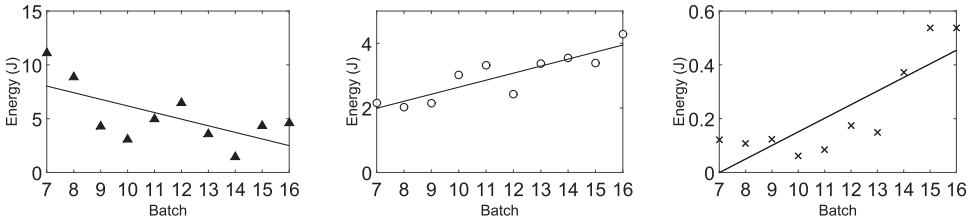

(a) MFCs with CEM at 1kΩ load Linear trend-line, y = -0.62x + 12.3

(b) MFCs with latex membrane at 3kΩ load Linear trend-line, y = 0.22x + 0.46

(c) MFCs with Tangoplus membrane at 13kΩ load Linear trend-line, y = 0.05x + 0.35

Fig. 5. Average energy output from MFCs over ten consecutive batch feeds under optimised load conditions.

different internal resistances within all study populations in at least one of the two polarisation experiments. For consistency within the experiment, a single optimum resistance value was approximated from polarisation data and applied to the whole group. Significant variation highlights the need for larger study populations to characterise the generalised behaviour of each membrane type. Due to the biological nature of the MFCs, some variation can be expected in system performance which may be effected by factors such as bacterial colonisation of the anode.

In contrast to the other membranes, the performance of MFCs with Tangoplus membranes was lower when placed under long term load at 13 kΩ (peak power = 0.92 μW, average of 10 batches, with the highest (1.83 μW, occurring in batch 14) during batches 7 onwards, than during batches 5 to 6 at 4 kΩ , but higher than during batches 1 to 4 at 1 kΩ (Table 1). This suggested the electrical characteristics of MFCs had changed during the course of the experiment and that the stratified load selected using the maximum power points on the polarisation curves was not the optimal load condition for power transfer from these MFCs. Hence, better characterisation of the optimal load condition could lead to better system performance. However, MFCs with Tangoplus showed the steepest temporal increase in energy produced per batch feed indicating that further development of the systems could increase power output (Fig. 5(c)). In contrast to both other membranes MFCs with Tangoplus showed consistent output between replicate systems. Average energy and maximum power output from MFCs with Tangoplus membranes had the lowest standard deviation under all load regimes. The most consistent performance of two replicate MFC types is shown by systems with Tangoplus during the polarisation experiment at 106 days (Fig. 6(b)). Furthermore, compared with the large change in power output, corresponding to small change in load, shown by the other MFCs, those with Tangoplus produced relatively stable power output over a larger load range of 4–13 kΩ. This stability of material performance is valuable in the design of MFC systems required to cope with varying load, which is a prevalent feature of real electrical systems.

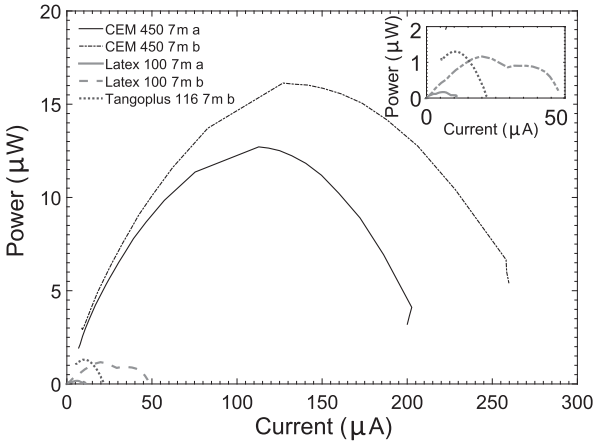

(a) Polarisation curve, at 79 days, following 1kΩ temporal loading

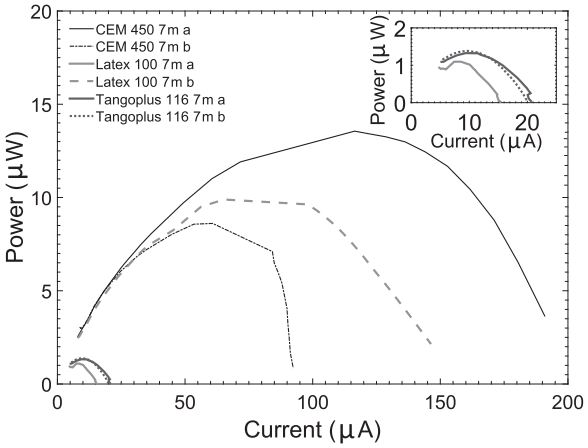

(b) Polarisation curve, at 106 days, following 4kΩ temporal loading

Fig. 6. Polarisation experiments at (a) 79 and (b) 106 days. Inset graphs show zoomed plot of Tangoplus and latex curves. Tangoplus a omitted from (a) due to negligible power output as shown in Table 2. Power value at each load is the average of all measurements taken at that load.

3.4. pH and conductivity of anolyte

Table 3 shows the pH and conductivity of the anolyte at the beginning and end of the final batch feed (batch 16). With the exception of one of the MFCs with Tangoplus membrane, whose anolyte had the same pH as at day 0, all MFCs show a higher anolyte pH at day 9 of batch 16 than at day 0.

Similarly, while the conductivity of the anolyte is higher at the end of the batch feed than at the start in most cases, the conductivity of the anolyte of MFC Tangoplus b is lower (39 μS). Fig. 7(a) shows the variation of power output with time across batches 12 to 16. The largest difference in power output throughout a single batch of any two MFCs of like membrane type in the investigation is shown by MFCs with CEM during batch 16 (Fig. 7(b)). This corresponds to the largest difference in the pH and conductivity of MFCs of like membrane type, at the end of the 9 days than either of the novel membrane types. This may have contributed to the difference in performance observed in MFCs with CEM.

Table 3
pH and conductivity of anolyte at 0 and 9 days of batch feed.

	0 days		9 days	
	pH	Conductivity	pH	Conductivity
CEM a	6.32	971 μS	6.46	1181 μS
CEM b	6.32	971 μS	7.24	2270 μS
Tangoplus a	6.32	971 μS	6.79	1057 μS
Tangoplus b	6.32	971 μS	6.32	932 μS
Latex a	6.32	971 μS	6.66	1290 μS
Latex b	6.32	971 μS	7	1322 μS

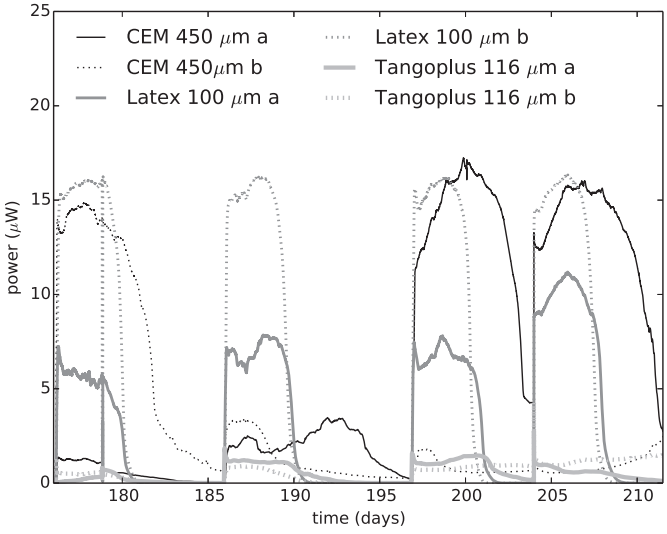

(a) Temporal power output from MFCs over batches 13 to 16

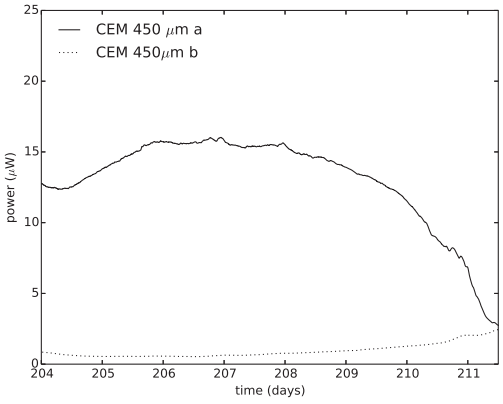

(b) Temporal power output from MFCs with CEM over batch 16

Fig. 7. Temporal power output over the duration of batch feeding.

3.5. Microscopy on membrane materials

Changes to the membrane material during operation could affect MFC performance either positively or negatively. Following operation, the surface of the CEM appears to be populated with round features that were not apparent prior to the material being used (Fig. 8(b)). This could be the result of biofouling of the surface, perhaps due to precipitation formed as a result of bacterial reactions. Previous studies have documented the deterioration of MFC performance due to increased MFC internal resistance caused by biofouling of the ion exchange membrane [17]. Hence, biofouling may have been a contributing factor of the temporal decrease in performance of the MFCs with CEM. In contrast to the CEM, the surface of latex appears to have actually degraded after it has been used as membrane in an MFC (Fig. 8(d)). Biodegradation of latex been observed concurrently with improved power output in previous work [15]. Biological action may have contributed to the temporal improvement in the performance of latex membranes observed in this study. However, the destructive nature of this process could also limit the lifespan of the MFC ultimately leading to membrane failure. There is less evidence of bacterial activity on the Tangoplus membranes following inclusion within the MFC compared to the other materials (Fig. 8(f)). This could suggest that the material is less prone to biodegradation and/or biofouling, which could contribute towards longevity and consistent performance.

Supplementary Fig. 1 shows cross sections of all membranes before and after experiments. CEM shows an increase in thickness of approximately 100 μm (s. Fig. 1(a) and (b)), suggesting that fluid from the anolyte was adsorbed by the material. A marginal increase in thickness is shown by the cross section of Tangoplus membranes (s. Fig. 1(e) and (f)) suggesting the absence of biodegradation of the material. Swelling due to fluid adsorption may be responsible for changing the surface topography of the dry material (Fig. 8(e) and (f)).

S. Fig. 1(c) shows latex membranes with a uniform thickness of 100 μm, prior to use in an MFC. S. Fig. 1(d) shows post–experiment images in which samples were significantly thinner than at the beginning of the experiment, with great variation in thickness across the sample. The reduction in thickness of the membrane suggests biodegradation of the material. This could be responsible for improved ionic transport between electrodes, therefore reducing losses in the MFC and increasing power output.

3.6. Cost

The cost of the raw materials required to produce each 20 cm^2 novel membrane was significantly lower than the cost of using the equivalent area of pre-fabricated CEM material. The cost of the natural rubber latex to produce one membrane was between £0.00075–0.0024 (USD 0.00112–0.00357) (Tomps) and the Tangoplus resin was £0.11 (USD 0.16) (Stratasys) compared to £0.15–0.27 (USD 0.22–40) for the equivalent area of CEM material. Therefore, both novel materials investigated present a cost effective solution to ion exchange membrane fabrication.

4. Conclusions

CEM produced the highest power and, consequently, energy of the three membranes considered. In contrast to MFCs with CEM, those with both novel polymers showed a strong trend of improved energy output. To our knowledge this study is the first to document 3D printed or k-bar drawn bio-polymer ion exchange membranes in an MFC. Facilitation of ionic conduction and electrical separation is clearly shown by both Tangoplus and natural rubber latex. Hence, the ionic conductivity, temporal improvement in performance, and power output of the same order of magnitude as conventional CEM (latex) and system stability and resistance to biological deterioration (Tangoplus) outweigh the significance of the inferior performance of these highly novel materials membranes, in the current setting.

The demonstration of 3D printable and castable materials as an MFC ion exchange surface verifies the possibility of rapid, low cost fabrication of MFCs with a significantly greater specific ion exchange area than planar membrane materials currently allow. Further investigation into the ionically conductive properties of materials available to these technologies will result in lower

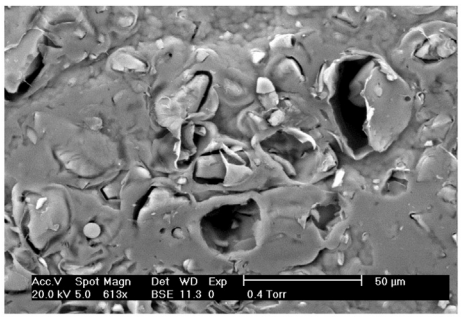

(a) CEM: Material surface pre-experiment

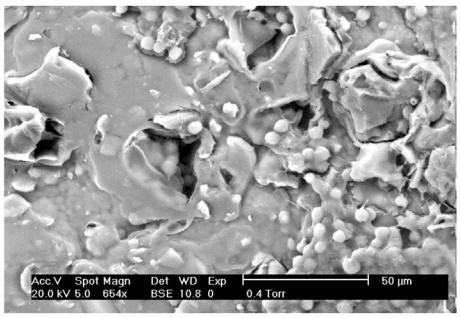

(b) CEM: Material surface post-experiment

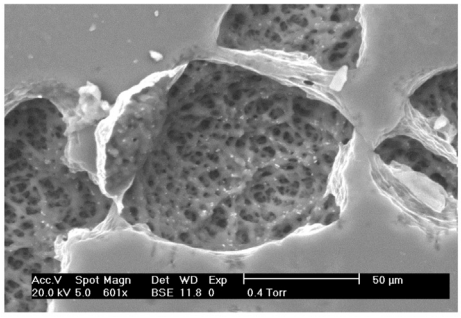

(c) Latex: Material surface pre-experiment

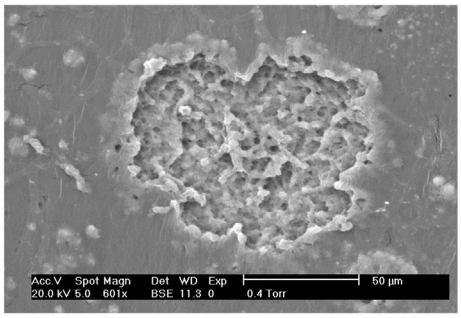

(d) Latex: Material surface post-experiment

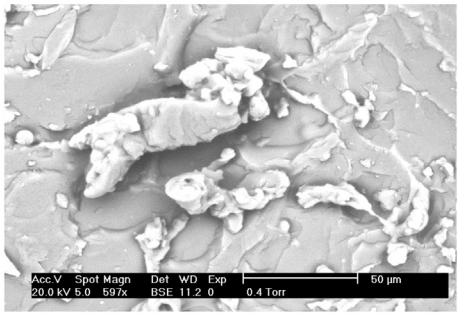

(e) Tangoplus: Material surface pre-experiment

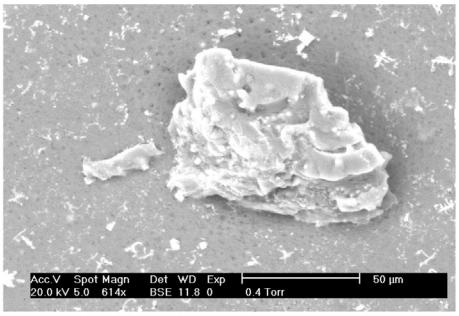

(f) Tangoplus: Material surface post-experiment (electrode material predominantly removed from surface)

Fig. 8. Membrane material on anode side of MFC at 0 days (pre-experiment) and 210 days (post-experiment), 300x magnification, scale bar: 200 µm.

internal resistance and consequently higher power densities. A contributing factor in the lower performance of the latex and Tangoplus membranes is undoubtedly their novelty and consequential poor characterisation. Further work will be used to exploit the potential of these promising fabrication techniques by further characterising the materials considered here and exploring the suitability of other materials. 3D printed moulds and formers could also be used to shape compliant ion-conductive materials such as latex into more complex geometries. The results of the current experiment invite further investigation into using the entire anode chamber casing as a soft ion exchange surface. Comparatively low cost and ease of fabrication are clear driving factors for this future work.

Acknowledgements

This work was supported by the Engineering and Physical Sciences Research Council (EPSRC) [grant number EP/I032533/1] and the Leverhulme Trust [grant number RPG-362]. Support in the use of SEM was kindy provided by Dr David Patton. Loan of a 3D digital microscope (Hirox) was provided by the EPSRC Engineering Instrument Pool. Ioannis Ieropoulos is an EPSRC Career Acceleration Fellow (grant numbers EP/I004653/1 and EP/L002132/1).

Appendix A. Supplementary data

Supplementary data related to this article can be found at http://dx.doi.org/10.1016/j.jpowsour.2015.04.113.

References

[1] John P. Hurley, Lansing M. Prescott, Donald A. Klein. Microbiology. Wm. C. Brown Publishers, Dubuque, 3rd edition, ISBN: 0-697-29390-4.
[2] Ioannis Ieropoulos, John Greenman, Chris Melhuish, Microbial fuel cells based on carbon veil electrodes : Stack configuration and scalability (April), Int. J. Energy Res. (2008) 1228–1240, http://dx.doi.org/10.1002/er.
[3] Y. Zuo, S. Cheng, D. F Call, B. Logan, Scalable tubular membrane cathodes for microbial fuel cell applications, ACS Natl. Meet. Book Abstr. 41 (9) (2007)

3347–3353. ISSN 00657727.
[4] M.M. Ghangrekar, P.S. Jana, M. Behera, Effect of organic loading rates and proton exchange membrane surface area on the performance of an up-flow cylindrical microbial fuel cell, J. Environ. Sci. Eng. 54 (1) (2012) 1–9.
[5] Zhuwei Du, Haoran Li, Tingyue Gu, A state of the art review on microbial fuel cells: A promising technology for wastewater treatment and bioenergy, Biotechnol. Adv. 25 (5) (2007) 464–482, http://dx.doi.org/10.1016/j.biotechadv.2007.05.004. ISSN 0734-9750.
[6] Sang-eun Oh, Bruce E. Logan, Proton exchange membrane and electrode surface areas as factors that affect power generation in microbial fuel cells, Appl. Microbiol. Biotechnol. (2006) 162–169, http://dx.doi.org/10.1007/s00253-005-0066-y.
[7] Jonathan Winfield, Ioannis Ieropoulos, David Patton, Biodegradation and proton exchange using natural rubber in microbial fuel cells, Biodegradation 24 (6) (2013a) 733–739, http://dx.doi.org/10.1007/s10532-013-9621-x.
[8] Jonathan Winfield, Lily D. Chambers, Andrew Stinchcombe, Jonathan Rossiter, The power of glove : Soft microbial fuel cell for low-power electronics, J. Power Sources 249 (2014) 327–332, http://dx.doi.org/10.1016/j.jpowsour.2013.10.096.
[9] Manaswini Behera, Partha S. Jana, M.M. Ghangrekar, Performance evaluation of low cost microbial fuel cell fabricated using earthen pot with biotic and abiotic cathode, Bioresour. Technol. 101 (4) (February 2010) 1183–1189, http://dx.doi.org/10.1016/j.biortech.2009.07.089. ISSN 1873-2976.
[10] J.G. Liu, T.S. Zhao, Z.X. Liang, R. Chen, Effect of membrane thickness on the performance and efficiency of passive direct methanol fuel cells, J. Power Sources 153 (1) (January 2006) 61–67, http://dx.doi.org/10.1016/j.jpowsour.2005.03.190. ISSN 03787753.
[11] Mohsen Shahinpoor, Ionic polymerconductor composites as biomimetic sensors, robotic actuators and artificial musclesa review, Electrochimica Acta 48 (14–16) (June 2003) 2343–2353, http://dx.doi.org/10.1016/S0013-4686(03)00224-X. ISSN 00134686.
[12] Jonathan Rossiter, Peter Walters, Boyko Stoimenov, Printing 3D dielectric elastomer actuators for soft robotics, Proc. SPIE 7287 (2009) 1–10, http://dx.doi.org/10.1117/12.815746.
[13] Ioannis Ieropoulos, Chris Melhuish, John Greenman, Jonathan Winfield, Small scale microbial fuel cells and different ways of reporting output I. A. Ieropoulos, Trans. E C S Soc. Electrochem. 28 (9) (2010) 1–9.
[14] Chen Zhao, Caiyun Wang, Robert Gorkin, Stephen Beirne, Kewei Shu, Gordon G. Wallace, Three dimensional (3D) printed electrodes for interdigitated supercapacitors, Electrochem. Commun. 41 (April 2014) 20–23, http://dx.doi.org/10.1016/j.elecom.2014.01.013. ISSN 13882481.
[15] Jonathan Winfield, Ioannis Ieropoulos, Jonathan Rossiter, John Greenman, David Patton, Biodegradation and proton exchange using natural rubber in microbial fuel cells, Biodegradation 24 (6) (November 2013) 733–739, http://dx.doi.org/10.1007/s10532-013-9621-x. ISSN 1572-9729.
[16] Jonathan Winfield, Ioannis Ieropoulos, John Greenman, Julian Dennis, Investigating the effects of fluidic connection between microbial fuel cells, Bioprocess Biosyst. Eng. 34 (4) (May 2011) 477–484, http://dx.doi.org/10.1007/s00449-010-0491-x. ISSN 1615-7605.
[17] Juan Xu, Guo-Ping Sheng, Hong-Wei Luo, Wen-Wei Li, Long-Fei Wang, Han-Qing Yu, Fouling of proton exchange membrane (PEM) deteriorates the performance of microbial fuel cell, Water Res. 46 (2012) 1817–1824, http://dx.doi.org/10.1016/j.watres.2011.12.060. ISSN 00431354.